DOI: 10.15669/pnst.8.160

Progress in Nuclear Science and Technology
Volume 8 (2025) pp. 160-164

ARTICLE

Validation Study on SFR Core Bowing Codes using Joyo Ex-Core Experiment Data: Single Duct Bowing Benchmark

Kazuya OHGAMA [1], Norihiro DODA [1*], Hirokazu OHTA [2], Nicholas WOZNIAK [3], Tomoyuki UWABA [1], Satoshi FUTAGAMI [1], Masaaki TANAKA [1], Hidemasa YAMANO [1], Takanari OGATA [2], Emily SHEMON [3] and Bo FENG [3]

[1] *Japan Atomic Energy Agency, 4002 Narita, Oarai, Ibaraki, 311-1393, Japan*
[2] *Central Research Institute of Electric Power Industry, 2-6-1 Nagasaka, Yokosuka-shi, Kanagawa, 240-0196, Japan*
[3] *Argonne National Laboratory, 9700 S Cass Ave, Lemont, IL 60439, USA*

Core bowing reactivity is expected to be an important negative feedback effect during abnormal reactor power increases such as unprotected transient overpower and unprotected loss-of-flow events in sodium-cooled fast reactors. However, accurate evaluation of this reactivity remains a challenge because the phenomenon is caused by slight displacements of fuel assemblies, which are difficult to accurately predict. This study aims to ensure the reliability of core bowing analysis codes using single-duct ex-core thermal bowing experimental data. Under a United States-Japan cooperation, ANL, CRIEPI and JAEA conducted thermal bowing analyses of a single duct using their own core bowing analysis codes and compared their results with the measurements in the axial distribution of horizontal displacements of the duct due to thermal bowing and contact loads on duct pads. The analysis results using the three codes agreed well with each other and were consistent with the experimental results. This code validation study confirmed that the core bowing analysis codes could reasonably predict the thermal bowing of a single duct.

KEYWORDS: core bowing, code validation, reactivity feedback, Joyo ex-core experiment, SFR

I. Introduction

A reactivity change is induced due to thermal bowing of fuel assemblies due to variations in reactor power. This reactivity change is called core bowing reactivity and can potentially provide a negative feedback effect during abnormal reactor power increases such as unprotected transient overpower and unprotected loss of flow events in sodium-cooled fast reactors (SFRs). The core bowing reactivity, which is given by complex phenomena of neutronics, thermal-hydraulics, and structural mechanics, involves larger uncertainties in its evaluation compared to those of the other reactivity feedbacks in SFRs. To develop a reliable evaluation methodology of the core bowing reactivity, a study of structural mechanics analysis for assembly thermal bowing and the irradiation effects such as swelling and creep is indispensable because the development of codes and verification and validation (V&V) studies for them are very limited unlike other phenomena such as neutronics and thermal-hydraulics. As a beginning of V&V effort, this study focused on the V&V of the thermal bowing model. A V&V study for thermal bowing of a single duct and groups of ducts was conducted as an international benchmark in the framework of the International Working Group on Fast Reactor (IWGFR).[1,2] The IWGFR benchmark included analyses of two single-duct experiments (one single duct with a constraint system and one without the constraint) and one multi-duct experiment provided by Japan Atomic Energy Agency (JAEA) as thermal bowing validation problems. Because these experiments were conducted with hexagonal ducts with the same dimensions of wrapper tubes of fuel assemblies of the experimental fast reactor Joyo as a part of its development, they are called Joyo ex-core thermal bowing experiments. However, it is not sufficient to examine the accuracy of a structural mechanics analysis model with very limited experiments mentioned above. Therefore, JAEA investigated records and re-examined additional Joyo ex-core thermal bowing experiments including eight single duct experiments and nine multi-duct experiments, and working together with Argonne National Laboratory (ANL) and Central Research Institute of Electric Power Industry (CRIEPI) to conduct the validation study using their own core bowing analysis codes in a joint study between the U.S. and Japan. The validation studies are divided into two parts: single duct experiments and multi duct experiments, and this paper describes the analysis results of the single duct experiments.

II. Single Duct Bowing Experiment

As shown in **Fig. 1**, a single Joyo-type fuel assembly ductwas inserted into the connecting tube installed on the core support plate and restrained at the upper right and lower left positions. The bending stiffness of the fuel pin bundle is smaller than that of the duct, and the effect of the bundle bowing on the duct bowing is limited. Hence, this experiment focuses on the thermal bowing of the duct. **Table 1** shows the specifications of the single duct experiment equipment. The hexagonal duct bowed toward the right side due to differences in the degrees of thermal expansion of the left wall with the heater and its opposite parallel side wall due to the temperature gradient given by the heater equipped inside the duct. The duct bowing was limited by the upper and the lower

* Corresponding author, E-mail: doda.norihiro@jaea.go.jp

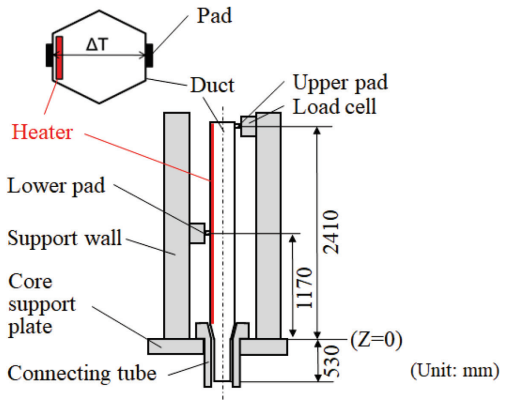

Fig. 1 Single duct experimental setup

Table 1 Assembly duct specifications

Items	Values	Unit
Duct total length	2970	mm
Elevation of upper /lower pads	2410/1170	mm
Hexagonal duct outer width	78.32	mm
Duct wall thickness	1.45	mm
Material of duct and pad	SUS316	-
Spring stiffness at upper pad	Very stiff	N/mm
Spring stiffness at lower pad	2.35×10^3	N/mm
Clearance at entrance nozzle	0.15	mm

pads. This experimental configuration simulates the actual assembly bowing in the core. The horizontal displacements due to the thermal bowing were measured at 10 axial points by a laser transit, and contact loads on the upper and the lower pads of the duct were measured by load cells. The experimental parameters were the initial gap widths between the pad and the load cell at the upper and the lower pad positions, and the differences in temperatures between the wall with the heater and its opposite parallel side wall.

III. Analysis Codes for SFR Core Bowing

To simulate the assembly thermal bowing, ANL, CRIEPI, and JAEA have respectively developed the analysis codes NUBOW-3D,[3] ARKAS,[4] and FINAS.[5] Their analytical model is shown in **Fig. 2**. They built the entire assembly length model using beam elements that can consider the bending stiffness and the circumferential temperature distribution of the duct. They employed contact elements to simulate the contacts of the lower and the upper pads with the left and the right support walls, respectively. In NUBOW-3D and FINAS, the contact of the bottom end of the entrance nozzle with the inner wall of the connecting tube is also represented by using the contact elements. Furthermore, the analysis model includes the inclination of the assembly by fixing both the horizontal and vertical displacements and allowing rotation at the axial position of the core support plate. ARKAS does not explicitly model the entrance nozzle but incorporates the equivalent rotational stiffness to simulate the same pivot support rotation.

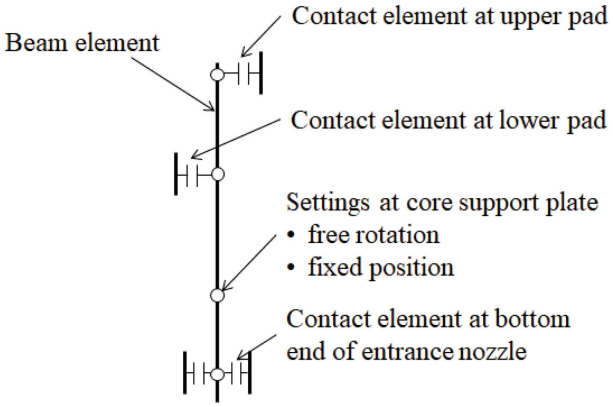

Fig. 2 Core bowing analysis model

IV. Analysis Results and Discussions

For the validation, 10 cases with different initial gaps at the upper and the lower pads and temperature distributions were prepared. The restraint conditions are characterized by the initial gap listed in **Table 2**. The initial gap widths at the upper and the lower pad positions in S6 and S7 were zero, and those

Table 2 Measured initial gap widths at the upper and the lower pad positions

Case	S1	S2	S3	S4	S5	S6	S7
Upper	1.2	3.05	3.05	3.05	3.05	0	0
Lower	1	0.8	0.8	0.8	0.8	0	0

(unit: mm)

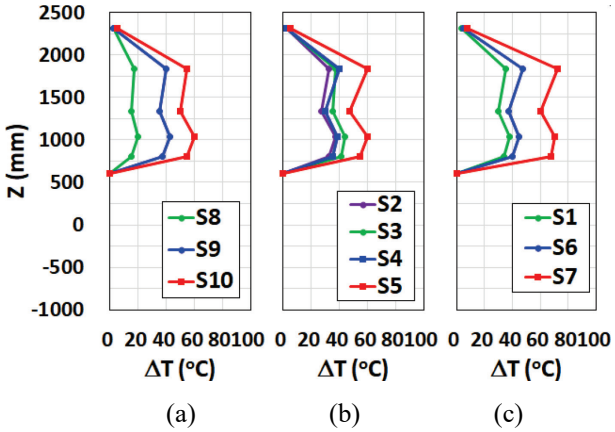

Fig. 3 Differences of measured temperatures between the wall with the heater and its opposite parallel side wall: (a) no constraint cases, (b) large initial gap cases, and (c) small/no initial gap cases

Table 3 Differences of measured temperatures between the wall with the heater and its opposite parallel side wall

Z (mm)	S1	S2	S3	S4	S5	S6	S7	S8	S9	S10
800	33.8	32.5	41.3	35	55	40	67.5	15	37.5	55
1040	37.8	37.5	43.7	38.8	60	45	70	20	42.5	60
1340	30	27.5	35	30	47.5	37.5	60	15	35	50
1840	35	32.5	37.5	40	60	47.5	72.5	17.5	40	55
2310	3.76	2.5	2.5	2.5	5	5	7.5	2.5	2.5	5

(unit: °C)

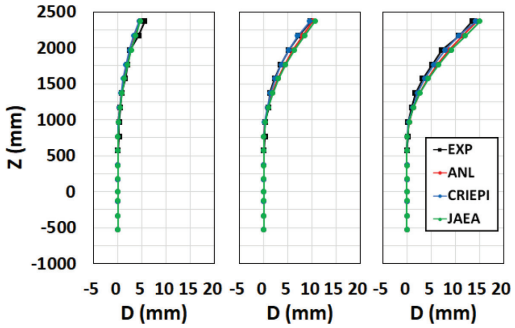

(a) S8 (b) S9 (c) S10

Fig. 4 Horizontal displacements of the duct in the no constrain cases (S8−S10)

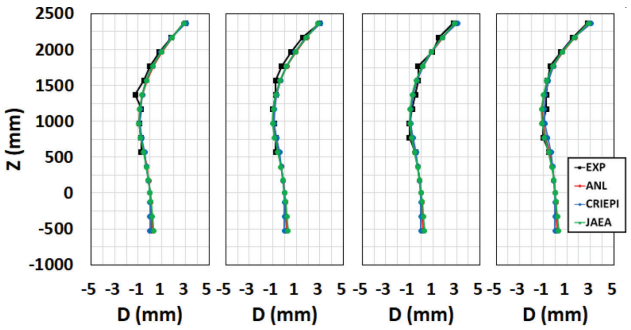

(a) S2 (b) S3 (c) S4 (c) S5

Fig. 5 Horizontal displacements of the duct in the large initial gap cases (S2−S5)

in S1 were as small as 1.2 mm. On the other hand, those in S2-S5 were 3.05 and 0.8 mm, respectively. In S8 to S10, the duct was not constrained. The zero gap condition closely simulates the actual state in the core, since a reactor core is designed to maintain the zero gap during rated operation.

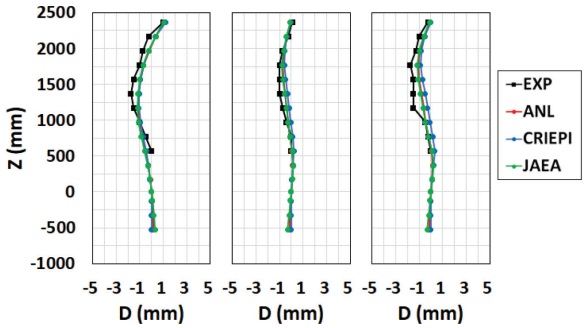

(a) S1 (b) S6 (c) S7

Fig. 6 Horizontal displacements of the duct in the small/no initial gap cases (S1, S6, and S7)

Differences of temperatures between the wall with the heater and its opposite parallel side wall were varied as shown in **Fig. 3** and **Table 3**. The test was conducted at room temperature. The duct temperature was measured on the center line of the wall surface.

Figures 4−6 show the analysis and experimental results of horizontal displacements (D) of the duct for three groups: the no constraint cases (free bowing), the large initial gap cases, and the small/no initial gap cases, respectively. In each experiment, horizontal displacements were measured at the axial positions of 570, 770, 970, 1170, 1370, 1570, 1770, 1970, 2170, and 2370 mm from the core support plate. **Table 4** shows the measured maximum displacement (D_{max}) in each case and Mean Absolute Error (MAE) calculated from the calculations and measurements:

$$MAE = \frac{1}{n}\sum_{i=1}^{n}|C_i - M_i| \quad (1)$$

where C is calculations, M is measurements, and n is sample size.

Table 4 Horizontal displacement due to thermal bowing

Case			S1	S2	S3	S4	S5	S6	S7	S8	S9	S10
Exp	D_{max}	(mm)	1.8	3.0	3.0	2.8	2.8	1.0	1.8	5.5	9.8	13.5
ANL	MAE	(mm)	0.4	0.2	0.2	0.2	0.1	0.2	0.4	0.3	0.4	0.7
	MAE/D_{max}	(%)	23	7	7	6	5	21	22	5	5	5
CRIEPI	MAE	(mm)	0.4	0.2	0.2	0.2	0.2	0.3	0.6	0.4	0.1	0.3
	MAE/D_{max}	(%)	23	6	7	7	6	33	36	7	1	2
JAEA	MAE	(mm)	0.4	0.2	0.2	0.2	0.1	0.2	0.3	0.2	0.6	0.9
	MAE/D_{max}	(%)	23	6	7	6	5	20	20	4	6	7

Table 5 Contact load at upper and lower pads

Case		S1		S2		S3		S4		S5		S6		S7	
		(N)	(%)	(N)	(%)	(N)	(%)	(N)	(%)	(N)	(%)	(N)	(%)	(N)	(%)
Exp	Upper	211	-	117	-	168	-	147	-	382	-	520	-	765	-
	Lower	443	-	249	-	365	-	318	-	811	-	1147	-	1736	-
ANL	Upper	189	-10	104	-11	174	4	140	-5	343	-10	438	-16	694	-9
	Lower	333	-25	152	-39	301	-17	231	-27	669	-18	922	-20	1472	-15
CRIEPI	Upper	206	-2	112	-4	190	13	121	-18	372	-3	481	-7	758	-1
	Lower	386	-13	188	-25	352	-4	209	-34	737	-9	1014	-12	1597	-8
JAEA	Upper	214	2	128	9	202	21	166	13	382	0	461	-11	734	-4
	Lower	412	-7	226	-9	387	6	311	-2	781	-4	954	-17	1545	-11

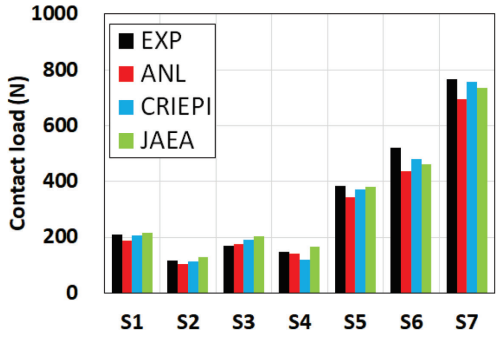

(a) Upper pad

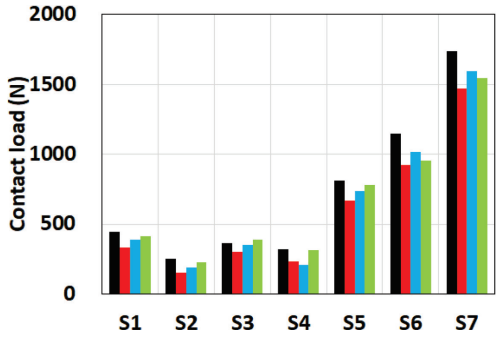

(b) Lower pad

Fig. 7 Contact load at pad

Figure 4 shows the comparison results of the assembly displacement in the no constraint cases (S8–S10). The assembly bowed freely, and the displacements became larger with the increase of the difference of temperature between the duct walls shown in Fig. 3 (a). The *MAEs* were within 10% of D_{max}, indicating that the three analysis codes could reproduce the measured displacement of the duct in the no constraint cases. For the initial gap cases (S2–S5), as shown in Fig. 5, the displacements were limited within approximately 3 mm at the upper pad position and 0.8 mm at the lower pad position, which were the initial gap widths. The *MAEs* were within 10% of the D_{max}, indicating that the three codes could reproduce the measured duct displacements.

The values of MAE/D_{max} in the small/no initial gap cases (S1, S6 and S7) are larger than those in other cases. However, it doesn't mean that the disagreement between the calculation and the measurement of the displacement was particularly large in these cases. These large values of MAE/D_{max} just came from the small D_{max} values. The averaged *MAEs* are 0.36 mm in these cases, 0.18 mm in S8–S10 and 0.43 mm in S2–S5, while the values of D_{max} are 1.0–1.8 mm, 5.5–13.5 mm and 2.8–3.0 mm in each case respectively. On the other hand, the relative differences in the contact loads in **Table 5** of the calculations and the measurements in these cases were same as or smaller than those of S2–S5.

Table 5 and **Figure 7** show the measured and the calculated contact loads at the upper and the lower pads in the cases of S1–S7. The calculated contact loads agreed with the experimental results within about 20% in the upper pad and within about 40% in the lower pad. The results indicate two trends on the relative differences between the calculations and the measurements. First, the relative differences of the contact loads in S2–S5 with the large initial gaps are generally larger than those in S6–S7 without the initial gaps. Secondly, the relative differences of the lower pad contact loads are larger than those in the upper pad contact loads. The maximum relative differences among the three organizations' calculations of the lower pad contact load are 17–39% in S2 and S5 and 15–25% in S6 and S7, while those of the upper pad contact loads are 10–21% in S2–S5 and 9–16% those in S6 and S7.

The measurement uncertainty of initial gaps is estimated to be one potential cause of the observed trends. The measurement uncertainty causes the differences between the measurements and the calculations of the contact loads, since each calculation was conducted by reflecting each corresponding measured initial gaps. Assuming that the model can reasonably predict contact loads, the measurement uncertainty of initial gaps causes and increases a disagreement between a measurement and a corresponding calculation.

Measurements of initial gaps were conducted with a gap gauge. Unfortunately, there is no information of the gap gauge used in the experiments and their measurement uncertainty in the record of the experiments. However, the measurements of the initial gaps of S6 and S7 were more reliable and reproducible than those of S2–S5, because the measurements of S6 and S7 were just confirming the tight contact of the pads and the load cells. As a result, the differences between the calculations and the measurements in S6 and S7 became smaller than those in S2–S5 with the initial gaps due to the relatively reliable initial gap values.

The reason for the larger differences in the lower pad

contact loads than those in the upper pad contact loads is estimated to be the bowing mode and the initial gap uncertainty. As shown in the no constrain free bowing cases in Fig. 4, the values of D_{max} are 10 mm in S9 under the condition of the maximum temperature difference (ΔT_{max}) of 45 °C and 13.5 mm in S10 under ΔT_{max} of 60 °C at the upper pad position. In the cases of S2−S5 under ΔT_{max} of 37.5−60 °C, displacements can be potentially same as those of S9−S10, if the duct is not constrained. On the other hand, the displacements at the lower pad are not expected to be large even if the duct is not constrained. Because of this difference in the potential displacements at the upper and the lower pad positions, the measurement uncertainty of the initial gap at the lower pad position is more sensitive to the calculation of the contact load than that at the upper pad position.

Through this validation study, it was confirmed that the analysis results of the horizontal displacements and the contact loads by the three codes agreed well with each other and were consistent with the experimental results. This study proves that the three codes can reasonably predict the thermal bowing of single duct.

IV. Conclusion

ANL, CRIEPI, and JAEA conducted the validation study of their own core bowing codes by using the Joyo ex-core experimental data and compared their analysis results with the measurements. For the single duct experiments, the analysis results by the three codes for the horizontal displacements and the contact loads agreed well with each other and were consistent with the experimental results. The code validation study using the single duct experiments confirmed that the core bowing analysis codes could reasonably predict the thermal bowing of a single duct.

Acknowledgment

JAEA and CRIEPI's works include the results of the "Technical development program on a fast reactor for demonstration (Program Grant Number JPMT007143)" ensured to JAEA by the Ministry of Economy, Trade and Industry in Japan (METI). The JAEA authors thank M. Iida of NESI Inc. for his assistance with the computational work.

Argonne's work was funded by the U.S. Department of Energy Office of Nuclear Energy's (DOE-NE) Fast Reactor Program (FRP). The submitted manuscript has been created by UChicago Argonne, LLC, Operator of Argonne National Laboratory ("Argonne"). Argonne, a U.S. Department of Energy Office of Science laboratory, is operated under Contract No. DE-AC02-06CH11357. The U.S. government retains for itself, and others acting on its behalf, a paid-up nonexclusive, irrevocable worldwide license in said article to reproduce, prepare derivative works, distribute copies to the public, and perform publicly and display publicly, by or on behalf of the Government. The Department of Energy will provide public access to these results of federally sponsored research in accordance with the DOE Public Access Plan. http://energy.gov/downloads/doe-public-access-plan.

References

1) International Atomic Energy Agency, "Verification and validation of LMFBR static core mechanics codes part I," IWGFR/75, 1990.
2) International Atomic Energy Agency, "Verification and validation of LMFBR static core mechanics codes part II," IWGFR/76, 1990.
3) G. A. McLennan, T. J. Moran, B. K. Cha, "Core structural analysis codes verification/qualification.[LMFBR]," *Trans. Am. Nucl. Soc.*, **30**, CONF-7811109-, (1978).
4) M. Nakagawa, "ARKAS: A three-dimensional finite element program for the core-wide mechanical analysis of liquid-metal fast breeder reactor cores," *Nuclear Technology*, **75**[1], 46-65 (1986).
5) K. Iwata,"General purpose nonlinear program FINAS for elevated temperature design of FBR components," *ASME Pressure Vessel and Piping Conference*, **66**, 119-137 (1982).